

α spectrin is essential for morphogenesis and body wall muscle formation in *Caenorhabditis elegans*

Kenneth R. Norman and Donald G. Moerman

Department of Zoology, University of British Columbia, Vancouver, BC, Canada V6T 1Z4

A common feature of multicellular animals is the ubiquitous presence of the spectrin cytoskeleton. Although discovered over 30 yr ago, the function of spectrin in nonerythrocytes has remained elusive. We have found that the *spc-1* gene encodes the only α spectrin gene in the *Caenorhabditis elegans* genome. During embryogenesis, α spectrin localizes to the cell membrane in most if not all cells, starting at the first cell stage. Interestingly, this localization is dependent on β spectrin but not β_{Heavy} spectrin. Furthermore, analysis of *spc-1* mutants indicates that β spectrin requires α spectrin to be stably recruited to the cell

membrane. Animals lacking functional α spectrin fail to complete embryonic elongation and die just after hatching. These mutant animals have defects in the organization of the hypodermal apical actin cytoskeleton that is required for elongation. In addition, we find that the process of elongation is required for the proper differentiation of the body wall muscle. Specifically, when compared with myofilaments in wild-type animals the myofilaments of the body wall muscle in mutant animals are abnormally oriented relative to the longitudinal axis of the embryo, and the body wall muscle cells do not undergo normal cell shape changes.

Introduction

The spectrin-based membrane cytoskeleton is a ubiquitous structure found in all metazoans examined. Members of the spectrin gene family and their associated proteins are widely distributed in most tissues in both vertebrates and invertebrates (Bennett and Baines, 2001). The spectrin molecule is a rod-shaped tetramer composed of two α and two β subunits (Bennett and Baines, 2001). Each subunit consists of a series of homologous 106 amino acid spectrin repeats, and nonrepetitive sequences are found in each subunit that could direct additional protein interactions. For example, the α spectrin molecule contains an SH3 domain and two EF hand Ca^{2+} binding domains. β spectrin contains an actin binding domain and a pleckstrin homology domain.

The spectrin-based membrane cytoskeleton was first characterized in erythrocytes and has subsequently been studied in great detail. In the erythrocyte, spectrin forms a submembrane cytoskeletal network that is important for maintaining the structural integrity of the membrane and maintaining cell shape (Lux and Palek, 1995). However, the role of the spectrin-based membrane cytoskeleton in nonerythrocytes has remained elusive. Studies in *Drosophila* and *Caenorhabditis elegans* are providing new information on the function of the

spectrin cytoskeleton in nonerythrocytes. In *Drosophila* and *C. elegans*, three spectrin genes have been identified. One gene encodes an α spectrin, and the other two genes encode β spectrins. The α and one of the β spectrins are highly similar to the nonerythroid spectrins (Dubreuil et al., 1987; Moorthy et al., 2000). However, the other β spectrin, β_{Heavy} (β_{H})* spectrin, is unusual in that it encodes a very large spectrin molecule ~ 400 kD (Dubreuil et al., 1990; Thomas and Kiehart, 1994; McKeown et al., 1998) compared with the nonerythroid β spectrin, which is ~ 220 kD (Dubreuil et al., 1987). In *Drosophila*, α and β spectrin are widely expressed in most tissues (Pesacreta et al., 1989). Conversely, the β_{H} isoform is restricted to certain tissues, such as the epithelia (Pesacreta et al., 1989; Thomas and Kiehart, 1994). Similarly, *C. elegans* β spectrin is found in most tissues (Moorthy et al., 2000), whereas the *C. elegans* β_{H} spectrin is restricted to the epidermis (hypodermis), pharynx, and intestine (McKeown et al., 1998). In *Drosophila* epithelial tissues, two spectrin isoforms associate with different membrane domains: the $(\alpha\beta)_2$ isoform localizes to the lateral and basal membrane, and the $(\alpha\beta_{\text{H}})_2$ isoform localizes to the apical membrane (Dubreuil et al., 1997).

Examination of *Drosophila* α spectrin mutants reveals several developmental defects, which implicate spectrin in the

Address correspondence to Donald G. Moerman, Dept. of Zoology, University of British Columbia, 6270 University Blvd., Vancouver, BC, Canada V6T 1Z4. Tel.: (604) 822-3365. Fax: (604) 822-2416. E-mail: moerman@zoology.ubc.ca

Key words: actin cytoskeleton; spectrin; morphogenesis; epithelia; muscle

*Abbreviations used in this paper: β_{H} , β_{Heavy} ; dsRNA, double-stranded RNA; Pat, paralyzed and arrested at the twofold stage; RNAi, RNA-mediated interference.

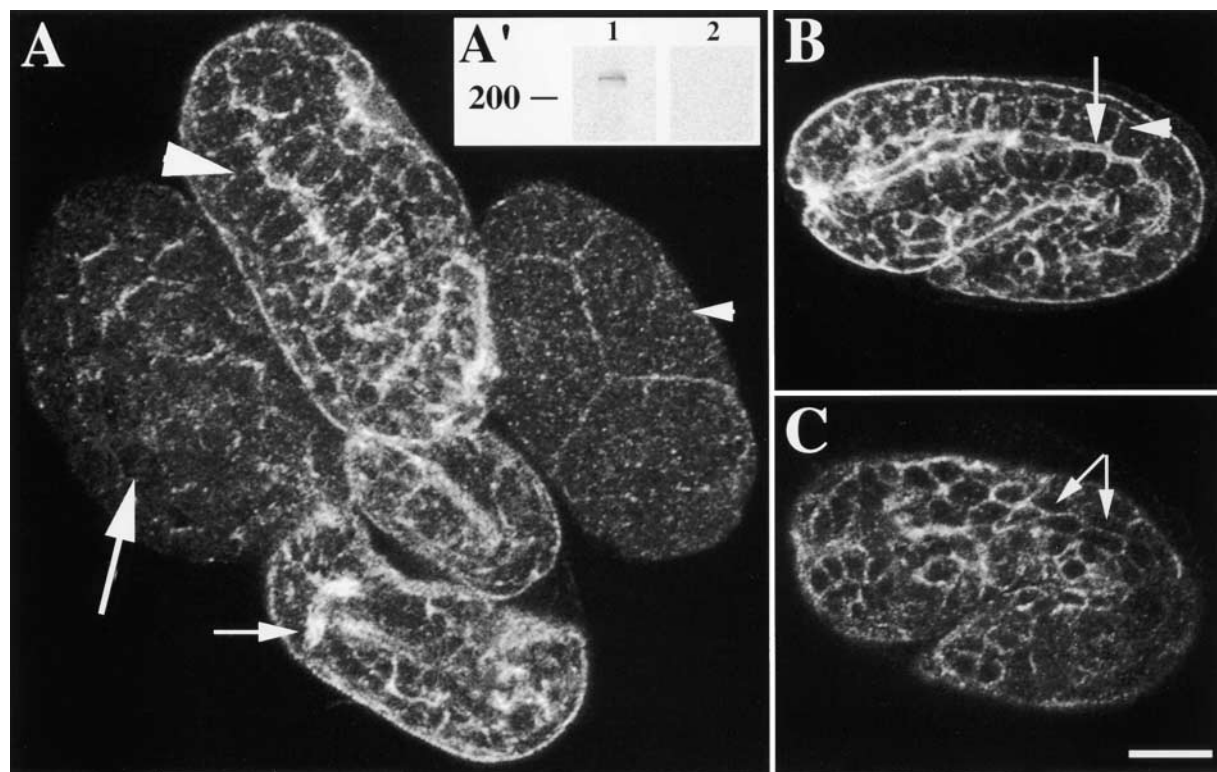


Figure 2. α spectrin localizes to the cell membrane of most cells during embryogenesis. (A) Four representative wild-type embryos at different developmental stages labeled with AS1 and examined by confocal immunofluorescence microscopy. The small arrowhead indicates a four-cell stage embryo where a spectrin is localized to the cell junctions. An \sim 100-cell stage embryo is shown with the large arrow; note cell membrane immunofluorescence. The large arrowhead indicates intestinal localization of a spectrin in a comma stage embryo. α spectrin localization in the nervous system of a threefold embryo is indicated by the arrow. (A') Western blot analysis of a mixed population of wild-type animals. Lane 1 indicates a \sim 240-kD band recognized by AS1 on wild-type worm extracts. (Lane 2) Preincubation of AS1 with the GST- α spectrin fusion protein shows no reactivity to wild-type worm extracts. (B) A representative 1.5-fold embryo labeled with AS1. Basolateral and apical localization of a spectrin is shown. Arrow indicates apical region, and the arrowhead indicates basolateral region of the intestine. (C) The body wall muscle cells (identified by counter staining with myosin antibody [unpublished data]) of a representative 1.5-fold embryo are outlined by a spectrin (arrows). Bar, 10 μ M.

processes of cell growth, differentiation, and specification (de Cuevas et al., 1996; Lee et al., 1997a; Thomas et al., 1998). Examination of β spectrin mutant animals in *Drosophila* and *C. elegans* implicate this molecule in body wall muscle function, axon pathfinding, synapse function, and the maintenance of protein localization at the membrane (Dubreuil et al., 2000; Hammarlund et al., 2000; Moorthy et al., 2000; Featherstone et al., 2001). β_H mutants have defects in cell morphological events including embryonic elongation of *C. elegans* embryos (McKeown et al., 1998) and epithelial morphogenesis in *Drosophila* oocyte development (Zarnescu and Thomas, 1999).

We have identified a mutation in the *C. elegans* α spectrin gene, *spc-1*. *C. elegans* α spectrin localizes to cell membranes in all tissues examined during embryogenesis. Phenotypic characterization of the *spc-1* mutant embryos reveals a defect in embryonic elongation and defects in body wall muscle differentiation. *spc-1* mutants have a slow rate of elongation and fail to elongate beyond twofold in length. This defect in elongation results from the failure of the apical actin cytoskeleton within the hypodermis to organize properly. Also, the body wall muscle displays an abnormal arrangement of myofilaments, and the body wall muscle quadrants are twofold wider than normal muscle quadrants. This wider partition-

ing is mirrored by the underlying basement membrane and in the hypodermal body wall muscle attachment structures. These results indicate that the spectrin-based membrane cytoskeleton is required for the normal development of these two tissues in *C. elegans*.

Results

C. elegans α spectrin is widely expressed throughout embryonic development

The *C. elegans* genome contains one α spectrin gene encoded by *spc-1* (*C. elegans* Sequencing Consortium, 1998). *spc-1* is composed of 13 exons (Fig. 1 A) and encodes a putative 2,421 amino acid protein containing 22 spectrin repeats, a central SH3 domain, and two EF hands located at the COOH terminus (Fig. 1 A). The *C. elegans* α spectrin is 61% identical and 76% similar to *Drosophila* α spectrin and 57% identical and 72% similar to the human nonerythroid α spectrin (Fig. 1 B).

To determine the localization of α spectrin in the developing embryo, a rabbit polyclonal antiserum was produced, designated AS1 (see Materials and methods). Wild-type embryos were stained with AS1 and examined by immunofluorescence microscopy. In early embryos, α spectrin is found

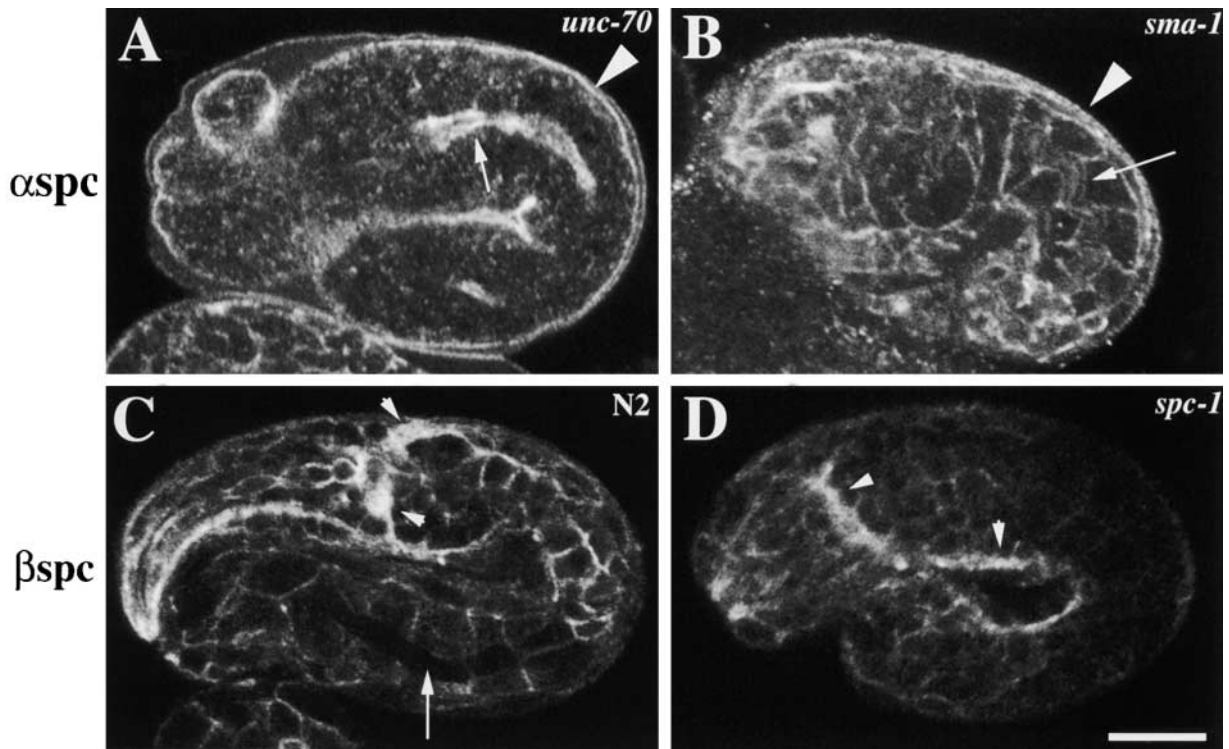


Figure 3. α and β spectrin localization in spectrin mutants. Representative (A) *unc-70(s1639)* and *sma-1(ru18)* (B) embryos labeled with AS1 and examined by confocal immunofluorescence microscopy. In *unc-70* (β spectrin) mutant embryos, (A) α spectrin fails to localize to the membrane except to the apical region of the intestine (arrow) and the hypodermis (arrowhead). (B) α spectrin localization is normal in *sma-1* (β_H spectrin) mutant embryos (the arrow indicates the apical region of the intestine, and the arrowhead indicates the apical region of the hypodermis). Wild-type (C) and *spc-1(ra409)* (D) embryos labeled with β spectrin antisera. (C) β spectrin localizes to the cell membrane of all cells including the nervous system (arrowheads). However, β spectrin does not localize to the apical region of the intestine (arrow) and hypodermis. (D) In the absence of α spectrin, β spectrin is not stably localized to the membrane as is seen by the faint immunofluorescence in the *spc-1* mutant embryo. However, stronger β spectrin immunofluorescence is detected in the nervous system of *spc-1* mutants (arrowheads). Bar, 10 μ M.

at or near the cell membrane in most if not all cells (Fig. 2) starting at the earliest stage of embryogenesis, indicating that α spectrin is maternally supplied (Fig. 2 A). After morphogenesis and organogenesis initiates, α spectrin localizes to the body wall muscle, hypodermis, pharynx, intestine, and developing nervous system (Fig. 2). In epithelial tissues, α spectrin is found at both the apical and basolateral regions of the membrane (Fig. 2 B). This is unlike the localization pattern observed for β spectrin, which is found in only the basolateral region of the membrane (Fig. 2 and Fig. 3 C) (Moorthy et al., 2000). With the exception of the apical regions, the localization of α spectrin overlaps with the distribution of β spectrin (Fig. 2 and Fig. 3 C) (Moorthy et al., 2000).

To determine specificity of AS1 antiserum, a putative α spectrin-null mutant (*spc-1[ra409]* [see below]) was stained with AS1. No signal was detected in *spc-1(ra409)* embryos except for faint immunofluorescence in the nervous system (unpublished data). Since α spectrin is maternally supplied, this faint labeling in the nervous system could be the result of maternal α spectrin. Using RNA-mediated interference (RNAi) of *spc-1* to disrupt maternal and zygotic α spectrin (Fire et al., 1998), α spectrin immunofluorescence was eliminated in early embryos, and no signal was detected in older embryos including the nervous system (unpublished data).

Furthermore, AS1 immunofluorescence was eliminated by preincubating the AS1 antiserum with the GST- α spectrin fusion protein but not with control fusion proteins (unpublished data). Additionally, Western blot analysis of a mixed population of wild-type worm extracts revealed a single band at \sim 240 kD (Fig. 2 A'). This band was not detected when AS1 antiserum was preincubated with the GST- α spectrin fusion protein (Fig. 2 A').

To determine if β spectrin is required for the localization of α spectrin, the localization of α spectrin was examined in β spectrin- and β_H spectrin-null mutants, *unc-70(s1639)* and *sma-1(ru18)*, respectively (McKeown et al., 1998; Hammarlund et al., 2000). In β spectrin mutants, α spectrin immunofluorescence is not observed in any tissues except for bright immunofluorescence in the apical membrane region of the intestine and hypodermis (Fig. 2 B and Fig. 3 A). Faint immunofluorescence is also observed in the nerve ring (unpublished data). Interestingly, this indicates that β spectrin is required for the localization of α spectrin in all tissues except the apical membrane in the hypodermis and intestine. Conversely, β_H spectrin was not required for the localization of α spectrin. In all tissues, α spectrin localized normally including the apical membrane region of the hypodermis and intestine (Fig. 3 B). To complement this analysis, α spectrin mutant embryos (see below) were stained

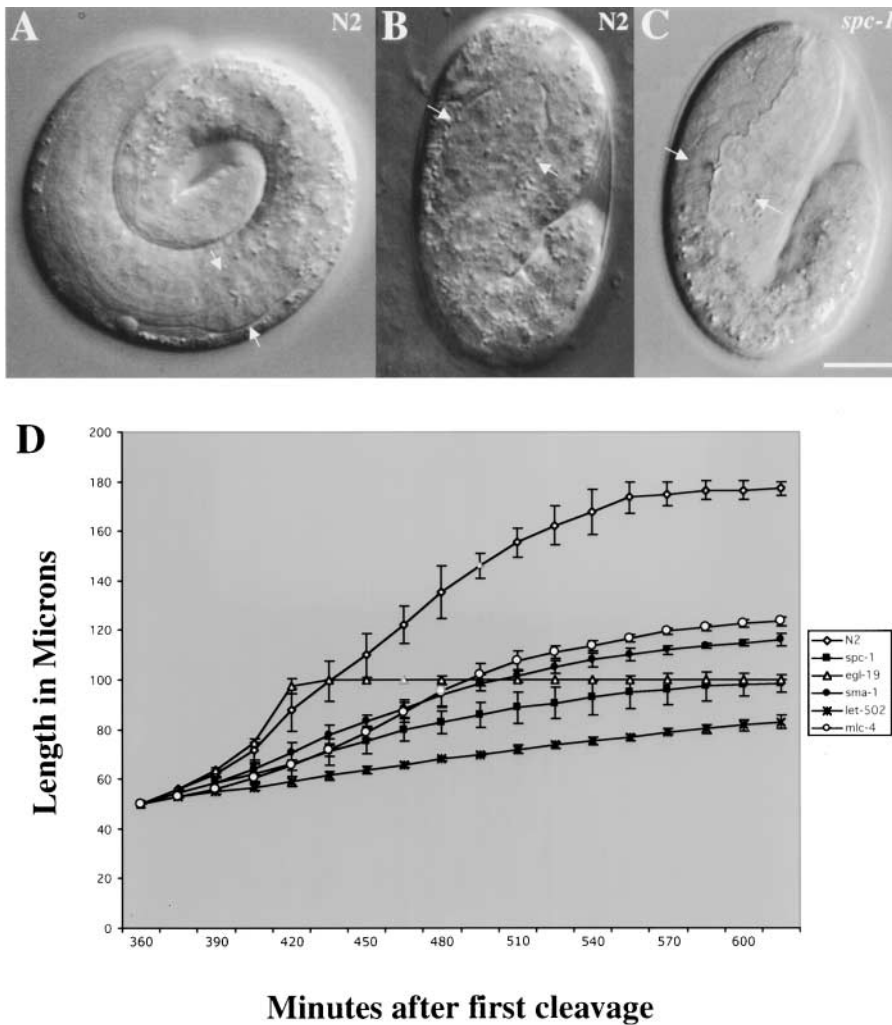


Figure 4. α spectrin is required for embryonic elongation. Nomarski images of representative wild-type (A and B) and *spc-1* (*ra409*) (C) embryos. (A) A wild-type embryo that has completed embryonic elongation (arrows indicate fully elongated pharynx). (B) A 1.5-fold wild-type embryo that has partially completed elongation (arrows indicate developing pharynx). (C) A *spc-1* mutant embryo at the same stage as the wild-type embryo shown in A. *spc-1* mutant embryos undergo elongation at a slower rate than wild-type animals and fail to complete elongation. Arrows indicate the abnormal morphology of the pharynx. Bar, 10 μ M. (D) Lengths of N2 ($n = 7$), *spc-1* ($n = 5$), *egl-19* ($n = 4$), *sma-1* ($n = 6$), *let-502* ($n = 5$), and *mlc-4* ($n = 4$) embryos measured every 15 min from first cleavage at 24°C. All the embryos initiated elongation at the same time. N2 and *egl-19* continue at the same rate until twofold in length where *egl-19* ceases elongation. *spc-1*, *sma-1*, *let-502*, and *mlc-4* undergo elongation at a slower rate. Additionally, body wall muscle contraction commenced at the same time (~ 400 min) in all the embryos except *egl-19*, which failed to display muscle contraction. Data is shown as the mean \pm SD.

with β spectrin antisera (Moorthy et al. 2000). In α spectrin mutants, β spectrin localized to the membrane; however, the staining was weak in all tissues except for the nervous system (Fig. 3 D). Surprisingly, this indicates that α spectrin is required for the stability but not the localization of β spectrin at the membrane.

Loss of α spectrin leads to a failure to complete embryonic elongation and lethality

In a mutagenesis screen designed to identify mutations in genes involved in body wall muscle development, an ethylmethanesulfonate-induced mutation in the *C. elegans* α spectrin gene was isolated. This mutation, *spc-1* (*ra409*), was genetically mapped to the left arm of the X chromosome between two cloned genes, *unc-2* and *unc-20*. Several approaches were used to determine that the *spc-1* (*ra409*) mutation is in the α spectrin gene. First, the *spc-1* (*ra409*) mutant phenotype was rescued by transformation rescue with a cosmid containing the full-length α spectrin gene (M01F12). Second, since this cosmid contained other genes, the *spc-1* (*ra409*) phenotype was rescued with a subclone of M01F12 containing only the α spectrin gene. Third, injection of double-stranded RNA (dsRNA) specific to the α spectrin coding region was found to phenocopy *spc-1* (*ra409*) mutants. Fourth, a transposon-induced allele of *spc-1* (*ra417*::

Tc1) (Fig. 1 A) fails to complement *spc-1* (*ra409*). Finally, by sequencing the entire α spectrin gene in *spc-1* (*ra409*) homozygotes the molecular lesion was identified, which introduces a premature stop at amino acid position 2111 (Fig. 1 A). To determine if *spc-1* (*ra409*) is a null mutation, it was crossed into a strain carrying a deficiency that deletes the *spc-1* locus (*syDf1*), and the heterozygous progeny were examined. *spc-1* (*ra409*)/*syDf1* progeny exhibited the same phenotype (described below) as *spc-1* (*ra409*) homozygotes, suggesting that *spc-1* (*ra409*) is a null allele of the *spc-1* locus.

To determine the role of α spectrin in embryogenesis, the phenotype of homozygous *spc-1* (*ra409*) mutant animals was analyzed using light microscopy. *spc-1* (*ra409*) mutant embryos undergo embryogenesis without any obvious defects until the embryo begins to elongate. Elongation converts the embryo from a ball of cells (lima bean stage) into the elongated threefold vermiform shape. Embryonic elongation is composed of two phases: (a) extension from lima bean to twofold, which is thought to occur by cell changes in the hypodermis, and (b) progressing from two to threefold, which is thought to be driven by body wall muscle contraction (Chin-Sang and Chisholm, 2000). *spc-1* (*ra409*) mutant embryos undergo elongation at a slower rate than wild-type animals during the first phase of elongation and fail to elongate beyond twofold in length (Fig. 4). In wild-type animals, it

Table I. Genetic interactions of spectrin

Genotype	Phenotype
<i>spc-1(ra409)</i>	Arrest as two fold L1 larvae
<i>spc-1(ra409)/+</i>	Wild type
<i>sma-1(ru18)</i>	Small viable animals
<i>sma-1(ru18)/+</i>	Wild type
<i>unc-70(n493n1171)</i>	Arrest as L1/2 larvae
<i>unc-70(n493n1171)/+</i>	Wild type
<i>unc-70(s1639)</i>	Arrest as L1/2 larvae
<i>sma-1(ru18)/+; spc-1(ra409)/+</i>	Wild type
<i>sma-1(ru18); spc-1(ra409)/+</i>	Small viable animals
<i>sma-1(ru18); spc-1(ra409)</i>	Arrest as two fold L1 larvae
<i>unc-70(n493n1171)/+; spc-1(ra409)/+</i>	Wild type
<i>unc-70(n493n1171); spc-1(ra409)</i>	Arrest as two fold L1 larvae
<i>unc-70(n493n1171) sma-1(ru18)/+</i>	Wild type
<i>unc-70(n493n1171)/+, sma-1(ru18)</i>	Unhealthy small semiviable animals
<i>unc-70(n493n1171), sma-1(ru18)</i>	Arrest as two fold L1 larvae

takes 60 min to extend to twofold. Conversely, in *spc-1* mutants it takes 180 min to extend to twofold. The resultant twofold embryos hatch but die soon after as small L1 larvae. Within the egg, *spc-1(ra409)* animals initiate body wall muscle contraction normally; however, their movement is not as vigorous as wild-type animals. Additionally, pharyngeal contraction is infrequent and irregular in *spc-1(ra409)* mutants. The pharynx in these mutant animals is much shorter than normal (Fig. 4, arrows). After hatching, *spc-1(ra409)* animals display muscle contraction, but their movement is uncoordinated.

To investigate whether other members of the spectrin cytoskeleton are involved in different developmental pathways, double mutants were constructed and analyzed for phenotypic enhancement. The series of double mutants constructed, which contain the different spectrin isoforms, *spc-1(ra409)* (α spectrin), *sma-1(ru18)* (β_H spectrin), and *unc-70(n493n1171)* (β spectrin), are listed in Table I. From this analysis, the only double mutant that displayed any enhancement in phenotype was the double homozygous animal with mutations in both β isoforms (genotype *unc-70(n493n1171), sma-1(ru18)*). These animals arrest development as L1 larvae that have failed to complete elongation, which is an identical mutant phenotype as homozygous *spc-1(ra409)* mutants (Table I). These results are consistent with and confirm a previous report that indicated that RNAi to both the β spectrin isoforms produced animals with the identical phenotype as *spc-1(RNAi)* animals (Moorthy et al., 2000). These data suggest that the spectrin cytoskeleton functions in two distinct developmental pathways, one pathway utilizes $(\alpha\beta_H)_2$ spectrin and the other $(\alpha\beta)_2$ utilizes spectrin.

The apical actin cytoskeleton of the hypodermis is disorganized in *spc-1* mutants

Since α spectrin mutants have defects in embryonic elongation, the mechanisms underlying elongation were investigated. In *C. elegans*, the process of embryonic elongation at least up to twofold is mediated solely by the contraction of actin bundles found on the apical surface of the hypodermis (Priess and Hirsh, 1986). These bundles are parallel to one another and circumferentially orientated around the embryo as visualized with fluorescent-labeled phalloidin (Fig. 5 A) (Priess and Hirsh, 1986; Costa et al., 1997). Compared with wild-type embryos, the hypodermal apical actin cytoskeleton

in α spectrin mutants is disorganized (Fig. 5 B). For example, several breaks along the length of the actin bundles can be observed, and the bundles are no longer held in a parallel arrangement (Fig. 5 B). To further investigate the role of the spectrin cytoskeleton in the organization of the hypodermal apical actin cytoskeleton, the organization of the actin cytoskeleton in the β spectrin mutants was investigated. *sma-1(ru18)* β_H spectrin and *unc-70(s1639)* β spectrin mutants were stained with fluorescent-labeled phalloidin and analyzed by confocal microscopy. The actin bundles are disorganized in β_H spectrin mutant animals (Fig. 5 C). As is seen with α spectrin mutants, there are several gaps in the actin filaments and they are not tightly organized in parallel bundles (Fig. 5 C). β_H spectrin mutants also have defects in elongation (McKeown et al., 1998). Although elongation is slower than normal in β_H spectrin mutants, these animals elongate further than α spectrin mutants (Fig. 4 D). Conversely, analysis of the *unc-70* β spectrin mutants revealed no defects in the hypodermal apical actin cytoskeleton (unpublished data). This indicates that β spectrin has no direct role in maintaining the integrity of the hypodermal apical actin cytoskeleton. Unlike the α spectrin and β_H spectrin mutants, β spectrin mutants do not have elongation defects. Therefore, it appears that $(\alpha\beta_H)_2$ and not $(\alpha\beta)_2$ spectrin is required for the organization and function of the hypodermal apical actin cytoskeleton during embryonic elongation.

A disorganized hypodermal apical actin cytoskeleton in α and β_H spectrin mutants can be explained by one of two possibilities. Either the disorganization of the apical actin cytoskeleton results in slow embryonic elongation or the lack of normal elongation results in the abnormal organization of the hypodermal apical actin cytoskeleton. To investigate the possibility of the latter, two mutants, *let-502(h738)* and *mlec-4(or253)*, that have a similar slow elongation phenotype (Fig. 4 D) were stained with fluorescent-labeled phalloidin and analyzed by confocal microscopy. *let-502* encodes a rho kinase, and *mlec-4* encodes a myosin light chain (Wissmann et al., 1997; Shelton et al., 1999). Both of these proteins have a putative role in the regulation of the contraction event required for embryonic elongation but not in actin assembly itself (Chin-Sang and Chisholm, 2000). The hypodermal apical actin cytoskeleton appears normal in both *let-502* and *mlec-4* mutants (Fig. 5, D and E). Interestingly, the spacing between the parallel actin bundles in *let-502(h738)* embryos appears irregular (Fig. 5 D). However, this is caused by the folding and wrinkling of the hypodermis in these mutants and not the structure of the actin bundles. Therefore, unlike the α and β_H spectrin mutants, *let-502* and *mlec-4* mutants display normal actin cytoskeleton organization. This suggests that the disorganization of the hypodermal apical actin cytoskeleton in α and β_H spectrin mutants is a direct result of the loss of the $(\alpha\beta_H)_2$ spectrin cytoskeleton and is not due to a defect in elongation.

Elongation is required for correct morphogenesis of the body wall muscle

During the analysis of the hypodermal cytoskeleton, abnormalities in the distribution of the thin filaments were observed in the body wall muscle of α spectrin mutant animals. This defect is not only associated with the thin filaments,

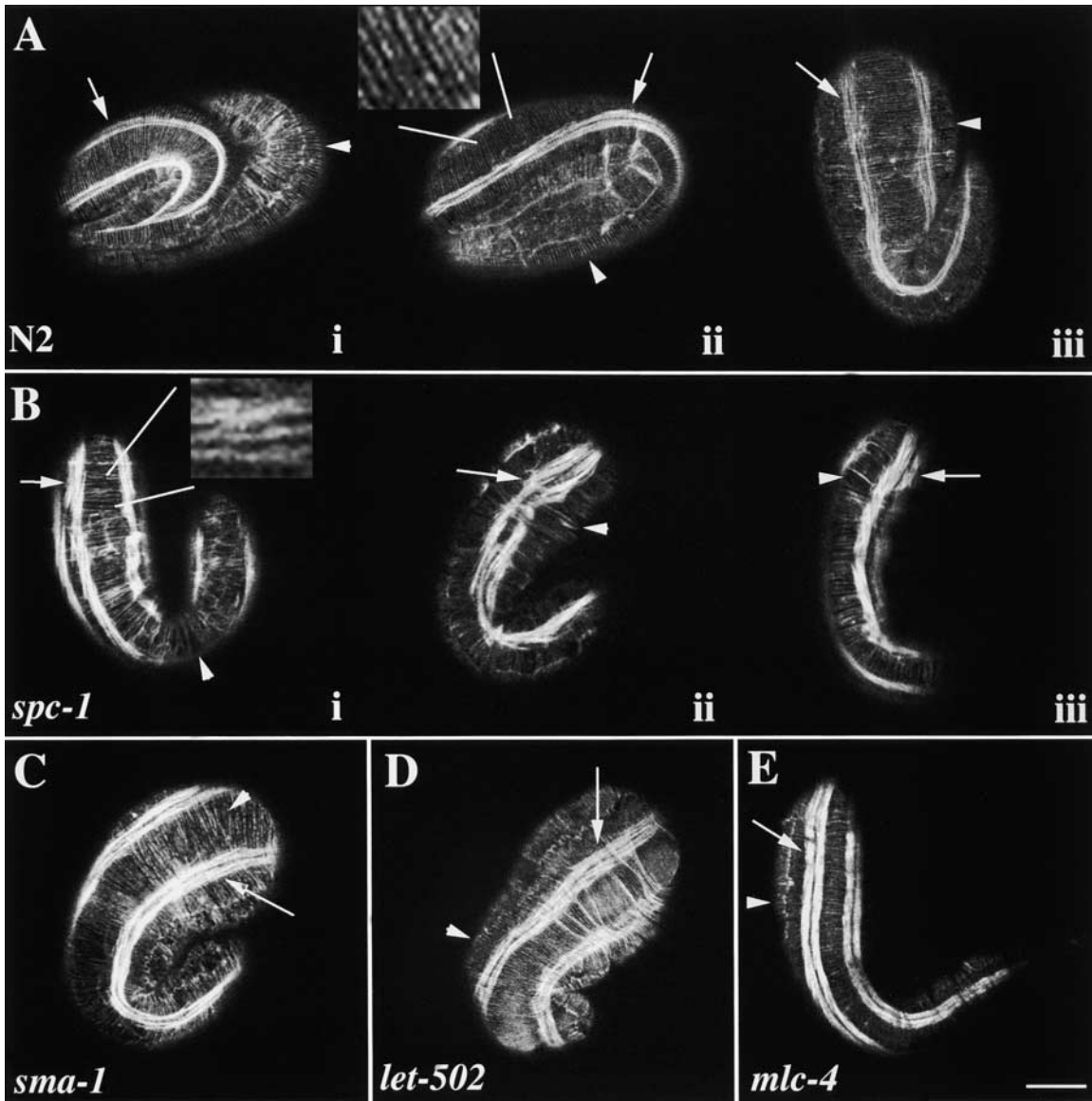


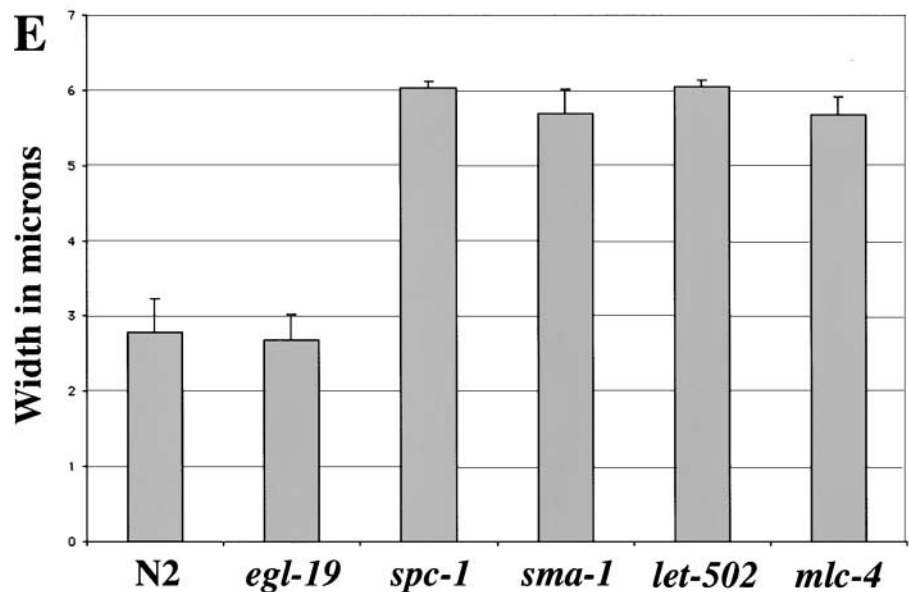
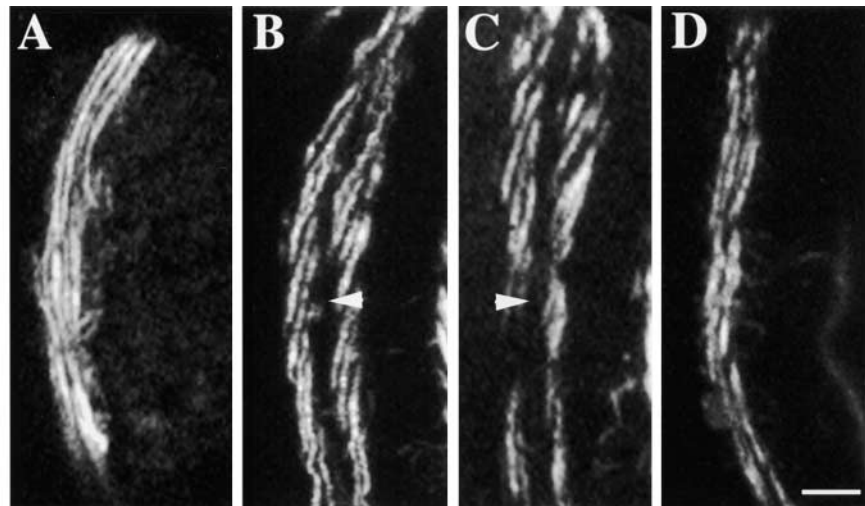
Figure 5. α spectrin is required for the organization of the hypodermal apical actin cytoskeleton. Representative wild-type (A), *spc-1*(*ra409*) (B), *sma-1*(*ru18*) (C), *let-502*(*h738*) (D), and *mlc-4*(*or253*) (E) embryos were stained with FITC-phalloidin and examined by confocal fluorescence microscopy to visualize the circumferentially oriented actin cytoskeleton in the hypodermis. Arrowheads indicate the circumferential actin fibers, and arrows indicate the thin filaments of the body wall muscle. In wild type (A), the actin filaments are organized in a circumferential pattern in parallel bundles (arrowheads) that run perpendicular to the body wall muscle quadrant (arrows). Ai and Aiii are threefold embryos (same developmental age as embryos shown in B–E, and Aiiii is a 1.5-fold embryo. The inset shows parallel organization of the actin fibers. In *spc-1* (α spectrin) embryos (B), several defects are observed in the highly regular pattern of the hypodermal actin cytoskeleton. Note the gaps (Bi and Biii, arrowheads), discontinuities, and clumping (Bii, arrowhead). Additionally, the thin filaments of *spc-1* mutant embryos are abnormally oriented, and the body wall muscle quadrants are wider than the muscle quadrants in wild-type animals (Bii and Aii, arrows). The inset highlights the disorganization of the actin fibers. (C) Although slightly less severe, similar defects are observed in *sma-1*(β_H spectrin) embryos. The arrowhead indicates a gap in the highly organized actin cytoskeleton. The hypodermal actin cytoskeleton in both *let-502* (D) and *mlc-4* (E) mutant embryos appears mostly wild type. In some instances, the spacing between some parallel actin bundles is abnormal in *let-502*(*h738*) embryos (see text). The same body wall muscle defect is observed in *sma-1*, *let-502*, and *mlc-4* mutant embryos that is observed in *spc-1* mutant embryos. All of these mutants have abnormally oriented thin filaments, and the body wall muscle is wider than normal (C and D, arrows). Bar, 10 μ M.

since similar defects are seen when the thick filaments of α spectrin mutants are examined by immunofluorescence microscopy with a monoclonal antibody specific to body wall muscle myosin. Specifically, the muscle quadrants of these mutants appear twofold wider than normal (Fig. 6, B and E). In addition, the myofilaments are abnormally oriented to the longitudinal axis. Normally, the sarcomeres are arranged at

an oblique angle (6°) to the longitudinal axis of the nematode (Fig. 6 A) (Waterston, 1988). In α spectrin mutants, this oblique striation is exaggerated to an almost 20° angle. This deflection of the sarcomeres is particularly prevalent in the anterior muscle cells (Fig. 6 B). Additionally, there is a large gap between the myofilament lattice in neighboring muscle cells within the same muscle quadrant that is not observed in mus-

Figure 6. Myosin filament organization is abnormal in elongation-defective mutants.

Representative wild-type (A), *spc-1(ra409)* (B), *sma-1(ru18)* (C), and *egl-19(st556)* (D) embryos were labeled with myosin antisera. The right dorsal muscle is shown in A–D, and anterior is up. In wild-type embryos (A), the myosin filaments are organized into a double row of A bands that runs approximately parallel with the longitudinal axis of the embryo. In both *spc-1* (α spectrin) (B) and *sma-1* (β_H spectrin) (C) mutant embryos, the myosin filaments are organized into double rows of A bands, but the filaments are abnormally oriented. The myosin filaments in these mutants are almost oriented at a 20° angle to the longitudinal axis of the embryo. Additionally, the muscle quadrants of the α (B) and β_H spectrin (C) mutant embryos are wider than normal (compare with A). Arrowheads in B and C indicate a large gap between the myofilament lattice in neighboring muscle cells. In *egl-19* mutants (D), the body wall muscle quadrants and the myofilaments are normal (compare with A). Bar, 5 μ M. (E) Width of the right dorsal muscle quadrant of N2 ($n = 6$), *egl-19* ($n = 5$), *spc-1* ($n = 6$), *sma-1* ($n = 5$), *let-502* ($n = 6$), and *mhc-4* ($n = 5$) embryos. The width of a muscle quadrant in wild-type animals is ~ 3 mm. Similarly, the muscle quadrants from the Pat mutant, *egl-19*, are ~ 3 - μ M wide. The slow elongation mutants, *spc-1*, *sma-1*, *let-502*, and *mhc-4*, all have muscle quadrants that are ~ 6 -mm wide. Data is shown as the mean \pm SD.



cle quadrants of wild-type animals (Fig. 5 B and Fig. 6 B). In wild-type animals, the myofilament lattice in neighboring cells is closely associated (Fig. 5 A and Fig. 6 A). In α spectrin mutant animals, the myofilament lattice is not tightly associated, and there is a 1–2 micron gap between the myofilament lattice in neighboring cells (Fig. 5 B and Fig. 6 B). This defect is not the result of the failure of the muscle cells to polarize, since the myofilaments are normally located against the basal membrane (unpublished data).

There are three possible causes for the morphological defects observed in the body wall muscle cells of α spectrin mutant animals: (a) loss of the spectrin cytoskeleton in muscle, (b) termination of elongation of the embryo at the twofold stage of development, or (c) a slow rate of elongation up to twofold. Since α and β spectrin are both expressed in body wall muscle and most likely form a complex, the myofilament lattice in β spectrin, *unc-70(s1639)*, mutant embryos was analyzed by immunofluorescence microscopy. From this analysis, the myofilament lattice of β spectrin mutants was indistinguishable from wild-type animals (unpublished data). This indicates that β

spectrin does not have a role in myofilament organization in the *C. elegans* embryo. Additionally, since α spectrin fails to associate with the membrane in the absence of β spectrin, this suggests that the alteration in body wall muscle cells of α spectrin mutants is not a direct result of loosening the muscle spectrin cytoskeleton. To investigate whether termination of elongation at twofold is itself the cause of the altered muscle, the paralyzed and arrested at the twofold stage (Pat) mutant, *egl-19(st556)*, was analyzed (Williams and Waterston, 1994). This mutant is defective for an L-type voltage-activated Ca^{2+} channel that is required for muscle contraction (Lee et al., 1997b). *egl-19* mutants initiate and undergo elongation normally until they reach twofold in length where elongation ceases (Fig. 4 D). Examination of the myofilaments in *egl-19* mutant embryos indicates that the myofilaments are normally assembled and organized (Fig. 6 D). Importantly, the width of the body wall muscle quadrants is identical to that of wild-type animals (Fig. 6 E). This demonstrates that the point where elongation ceases is not critical for the development of the body wall muscle. Interestingly, analysis of the slow elongation mutants, *sma-*

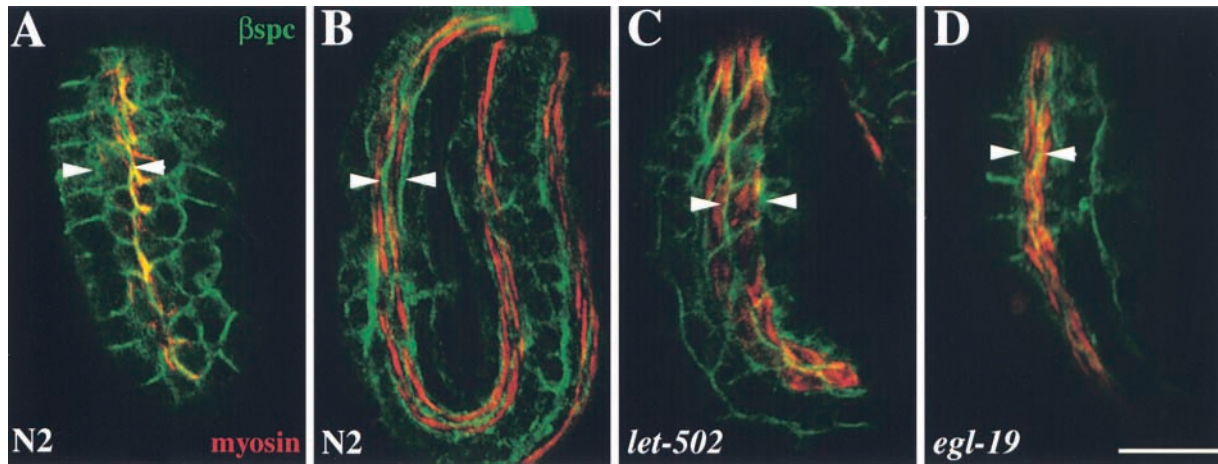


Figure 7. Body wall muscle cells fail to undergo cell shape changes in the slow elongation mutants. Representative wild-type (A and B), *let-502(h738)* (C), and *egl-19(st556)* (D) embryos double labeled with myosin antisera (red) and β spectrin antisera (green). In wild-type embryos, the body wall muscle cells change shape from round to spindle-shaped cells. (A) Comma stage wild-type embryo showing the initial shape of the body wall muscle cells at the start of embryonic elongation. (B) Threefold wild-type embryo indicating the cell shape change that the body wall muscle cells undergo during embryonic elongation. (C) In the slow elongation mutants (*let-502*), the body wall muscle cells fail to undergo normal cell shape changes and remain similar to the body wall muscle cells in the wild-type comma stage embryo (C compared with A and B). (D) Normal cell shape changes occur in the Pat mutant, *egl-19*. Arrowheads indicate cell width. Bar, 10 μ M.

$1(\beta_{\text{H}}$ spectrin), *let-502* (rho kinase), and *mlc-4* (myosin light chain), by fluorescence microscopy reveals that these mutants have the same body wall muscle phenotype as α spectrin mutants (Figs. 5 and 6). The muscle quadrants are twofold wider than normal, the myofilaments are abnormally positioned, and there is a large gap between the myofilament lattice in neighboring cells (Fig. 5, C–E, and Fig. 6, C and E). These data suggest that elongation from lima bean to twofold is critical for the normal development of the body wall muscle.

α spectrin, β_{H} spectrin, *let-502*, and *mlc-4* mutants have the same body wall muscle phenotype, and they have a slower rate of elongation than normal (Fig. 4 D) (McKeown et al., 1998). To examine whether a slower embryonic elongation up to twofold influences muscle cell shape, muscle cell changes during elongation were monitored. Wild-type and mutant embryos at various stages of elongation were examined with β spectrin and myosin immunofluorescence microscopy to visualize muscle cell shape changes. The cell shape changes that convert round body wall muscle cells into thin spindle-shaped cells were defective in the slow elongation mutants (Fig. 7). In these mutants, the muscle cells are square and have not lengthened (Fig. 7, B and C), but this process occurs normally in *egl-19* embryos even though these mutants only elongate to twofold (Fig. 7 D). Although *egl-19* mutants arrest elongation at twofold, these mutants elongate up to twofold at the same rate as wild-type embryos. These data indicate that the process of elongation from lima bean to twofold, not just the failure to elongate beyond, is critical for the normal development of the body wall muscle.

The basement membrane and hypodermal attachment structures are broader in slow elongation mutants

The body wall muscle is anchored to the cuticle via the basement membrane and hemidesmosomal-like components in the hypodermis (Moerman and Fire, 1997). Since the slow elongation mutants exhibit wider muscle quadrants, it is

possible that the basement membrane and the hemidesmosomal-like components exhibit defects also. To determine if any defects have arisen in the basement membrane, the distribution of the basement membrane protein perlecan was analyzed. The basement membrane of wild-type, α spectrin, β_{H} spectrin, *let-502*, and *egl-19* mutant embryos was assessed by perlecan immunofluorescence microscopy. Perlecan is an essential component of the basement membrane that is required to transmit the force of body wall muscle contraction to the hypodermis (Rogalski et al., 1993). The distribution of perlecan in α spectrin, β_{H} spectrin, and *let-502* mutant embryos matched the expansion of the body wall muscle quadrants and results in a wider basement membrane (Fig. 8, A–C). Aside from the larger size of the basement membrane, the distribution of perlecan appears wild type, and perlecan is evenly distributed under the muscle quadrant. The distribution of perlecan in *egl-19(st556)* was very similar to wild type, indicating that the basement membrane has not expanded in these mutants (Fig. 8 D).

To determine if similar alterations occur in the hemidesmosomal-like structures of the hypodermis, the organization of these attachment structures was investigated by using MH4 immunofluorescence. The MH4 antiserum recognizes intermediate filaments that are associated with hemidesmosomal-like structure in the hypodermis that assembles adjacent to the body wall muscle cells in the dorsal and ventral hypodermis (Francis and Waterston, 1991). In wild type, these hemidesmosomal-like structures resemble the spatial and temporal distribution of the muscle components and are tightly associated with the hypodermal membrane adjacent to the muscle cells where the myofilament lattice is positioned (Fig. 8 E) (Hresko et al., 1994). Although the spacing and organization of the hypodermal attachment structures appeared normal, MH4 immunofluorescence examination of the slow elongation mutants reveals that these structures closely mimic the expansion of the muscle cells (Fig. 8, F and G). This indicates

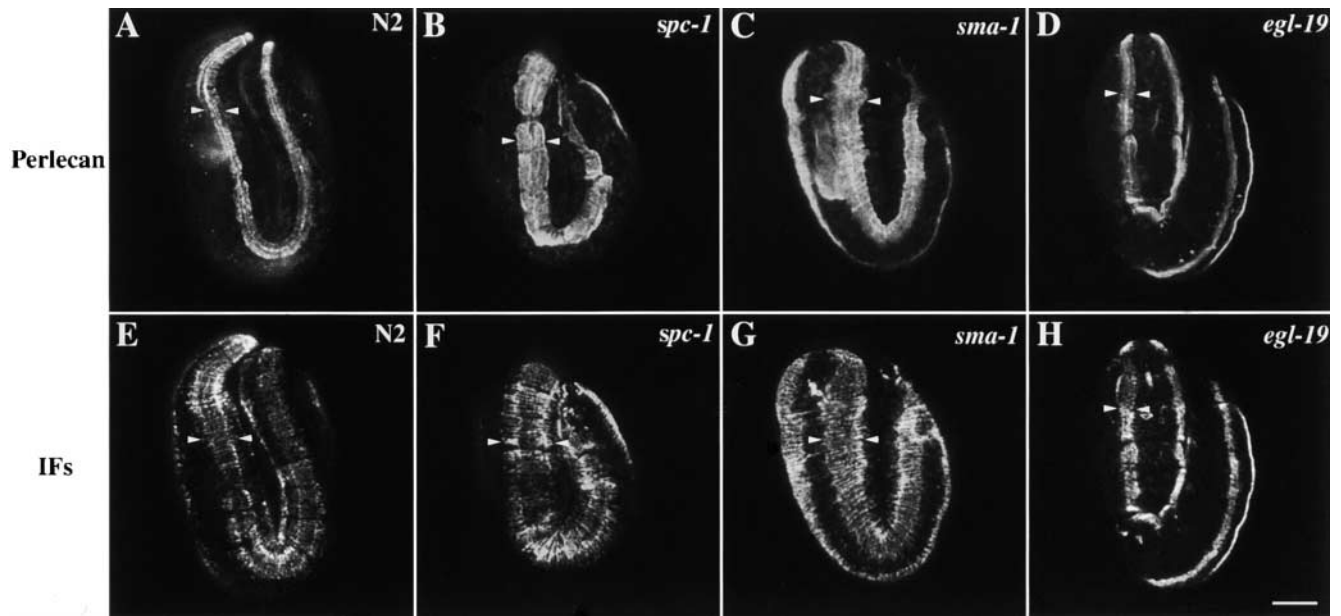


Figure 8. The basement membrane and hemidesmosomal-like structures have an expanded distribution in the slow elongation mutants. Representative wild-type (A and E), *spc-1*(*ra409*) (B and F), *sma-1*(*ru18*) (C and G), and *egl-19*(*st556*) (D and H) embryos double labeled with perlecan antisera and MH4, an antibody that recognizes the intermediate filaments of the hypodermal hemidesmosomal-like structure. In wild-type embryos (A), perlecan is evenly distributed under each of the body wall muscle quadrants. Similarly, in *spc-1* (α spectrin) (B) and *sma-1* (β_H spectrin) (C) mutants, perlecan is distributed evenly under each of the body wall muscle quadrants. However, the spatial distribution of perlecan in *spc-1* and *sma-1* mutants is wider than normal, reflecting the defects observed in the body wall muscle (Figs. 6 and 7). In *egl-19* mutants (D), the distribution of perlecan is normal. In wild-type embryos, the hemidesmosomes have assembled under each of the body wall muscle quadrants (E). In *spc-1* (F) and *sma-1* (G) mutant embryos, the hemidesmosomes have assembled normally under each body wall muscle quadrant (F and G). However, the hemidesmosomes are assembled in an area wider than normal. In *egl-19* mutants (H), the distribution of the hemidesmosomes is normal. Arrowheads indicate width of basement membrane (A–D) and hemidesmosomes (E–H). Bar, 10 μ M.

that the complete linkage from muscle to the cuticle is affected in these mutants. Analysis of MH4 distribution in *egl-19* reveals a wild-type pattern (Fig. 8 H).

Discussion

The *spc-1* locus of *C. elegans* encodes the ortholog of human nonerythroid α spectrin. During *C. elegans* embryogenesis, α spectrin localizes near the plasma membrane of most, if not all, cell types beginning at the first cell stage. During later stages of embryogenesis, α spectrin localizes to all tissues. This localization of α spectrin overlaps with β spectrin except in the apical membrane region of epithelial tissues. In the absence of β spectrin, α spectrin only localizes to the apical membrane region of epithelia, and small amounts are detected in the nerve ring. Conversely, although β spectrin appears to localize to the membrane in the absence of α spectrin, it is not stably localized. However, we did observe higher levels of β spectrin in the nervous system of *spc-1*(*ra409*) mutants, which is probably due to maternal contribution of α spectrin. Using a different experimental procedure, Moorthy et al. (2000) found normal levels of β spectrin in *spc-1*(*RNAi*) embryos (Moorthy et al., 2000). In our study, the genetic null was characterized, whereas Moorthy et al. (2000) examined RNAi-induced embryos. It is possible that RNAi produces a broad range of penetrance. In support of this hypothesis, when we used the same cDNA templates that Moorthy et al. (2000) used for dsRNA production we found that this resulted in a very mild defect, and only a small percentage of embryos phenocopied the *spc-*

I-null phenotype. Therefore, it is possible that in their analysis α spectrin was present, albeit in lower quantities, and allowed for normal β spectrin localization.

β_H spectrin has been reported to localize to the apical region of epithelial tissues in both *C. elegans* and *Drosophila* (Thomas, 2001) and therefore may be required for the apical localization of α spectrin. However, examination of α spectrin localization in β_H spectrin (*sma-1*) mutants reveals a normal distribution of α spectrin, indicating that β_H spectrin is not required for α spectrin localization in *C. elegans*. This suggests that the mechanisms that localize α spectrin to the apical versus the basolateral membrane are distinct.

The localization pattern of the different spectrin isoforms and the examination of α and β spectrin localization in the reciprocal mutants suggests that the spectrin cytoskeleton is organized into two populations: an $(\alpha\beta)_2$ spectrin that localizes to all tissues except the apical membrane in epithelia and an $(\alpha\beta_H)_2$ spectrin that localizes to the epithelial apical membrane. This model is further corroborated by the analysis of the double mutants (this study; Moorthy et al., 2000). Double mutants constructed with null alleles of β and β_H spectrin resulted in a phenotype identical to that of the single loss of function allele of α spectrin.

The $(\alpha\beta_H)_2$ spectrin cytoskeleton is essential for embryonic morphogenesis

Time-lapse video recording of α spectrin (*spc-1*) mutants during embryogenesis indicates that these mutants have a

slow rate of elongation resulting in L1 larvae that are half the size of wild-type L1 larvae. Circumferential contraction of the apically localized actin cytoskeleton in the hypodermis is the driving force behind the process of elongation during morphogenesis (Priess and Hirsh, 1986; Costa et al., 1997). Examination of this cytoskeleton in α spectrin mutants reveals that the actin filaments are discontinuous and disorganized. The same defect is observed in β_H spectrin mutants but is not observed in β spectrin mutant animals. Also, β_H spectrin mutants have defects in elongation, whereas β spectrin mutants do not. These data indicate that the $(\alpha\beta)_2$ spectrin cytoskeleton, and not $(\alpha\beta)_2$, is essential for the proper organization and function of the apical actin cytoskeleton in the hypodermis and is a key component involved in epithelial morphogenesis. The importance of the spectrin cytoskeleton in epithelial morphogenic events has been documented recently in *Drosophila*. Zarnescu and Thomas (1999) have shown that β_H spectrin is required for normal epithelial morphogenesis in *Drosophila* follicle cells during oocyte development. Additionally, spectrin has been implicated in morphogenic events that occur during mouse neural tube formation (Sadler et al., 1986) and during gastrulation in sea urchin embryos (Wessel and Chen, 1993). These observations together with our data suggest that the spectrin cytoskeleton may function globally in coordinating the cytoskeleton within epithelial tissues during morphogenic events.

The process of elongation occurs in two steps. First, the hypodermal apical actin cytoskeleton is required to extend the embryo to twofold, and second, body wall muscle contraction induces hypodermal cell changes that extend the embryo to threefold (Chin-Sang and Chisholm, 2000). Unlike Pat mutants, the elongation mutants described here (*spc-1*, *sma-1*, *let-502*, and *mlc-4*) are capable of muscle contraction and have a slow rate of elongation from lima bean to twofold. Pat mutants elongate to twofold normally, but they fail to elongate beyond twofold because their lack of muscle contraction fails to induce changes in the hypodermis. *spc-1*, *sma-1*, *let-502*, and *mlc-4* have defects in the hypodermal actin cytoskeleton and in extending to twofold. However, these mutants are capable of body wall muscle contraction. Presumably, the induction of hypodermal changes by body wall muscle contraction fails or is inefficient in these mutants because the completion of this induction event requires an intact hypodermal actin cytoskeleton, which is absent in these mutants.

Hypodermal-mediated contraction determines the shape of body wall muscle cells

Two lines of evidence indicate that the expression and function of α spectrin in the hypodermis, as opposed to spectrin expression within body wall muscle, is critical for determining the shape of the developing muscle cells. First, unlike α spectrin mutants, the β spectrin mutant, *unc-70*, does not have any defects in embryonic elongation or body wall muscle development. In β spectrin mutants, α spectrin fails to localize to the muscle cell membrane. These observations imply that spectrin expression within muscle is not important for determining muscle cell shape. Since *unc-70* mutants do not impede elongation, it appears that the presence

of spectrin within the hypodermis is sufficient for embryonic elongation to occur. A second line of evidence implicating the hypodermis in influencing muscle cell shape comes from the study of genes regulating the apical actin cytoskeleton. The genes we examined that influence the apical cytoskeleton with the exception of *spc-1*, including *let-502*, *sma-1*, and *mlc-4*, are expressed in the hypodermis but not in muscle (Wissmann et al., 1997; McKeown et al., 1998; Shelton et al., 1999). Mutants in all three genes elongate to twofold more slowly than wild-type embryos, and all three have broader muscles than wild-type embryos.

Embryonic elongation leads to a change in shape of the body wall muscle in wild-type embryos. A slower rate of elongation in the phase leading to a twofold embryo leads to a muscle cell with greater surface area in contact with the underlying hypodermis. Why a slower elongation rate leads to this final muscle cell shape is not clear. However, the consequences, a twofold increase in basement membrane in contact with the basal face of the muscle and a wider hemidesmosomal complex within the hypodermis, are quite dramatic. This is perhaps the most striking phenotype of these mutants and is what first drew our attention to the *spc-1* mutants.

During *C. elegans* embryogenesis, the myofilaments of muscle and the hypodermal hemidesmosomes assemble concurrently and have the same spatial distribution (Hresko et al., 1994). How the complementary patterning of hemidesmosomes and myofilament attachment sites is achieved is an intriguing problem in development. Does the pattern within muscle determine the pattern within the hypodermis, or is it the other way around? The hypodermis could direct the formation of the body wall muscle via the hemidesmosomal-like components that anchor the body wall muscle to the cuticle. Specifically, the hypodermal cytoskeletal rearrangements that are required for elongation could also be required to restrict hemidesmosomal placement. If these rearrangements are perturbed, this could lead to a wider distribution of the hemidesmosomes and result in wider muscle quadrants. Conversely, it is possible that the body wall muscle cells determine where the basement membrane and hypodermal hemidesmosomal-like structures are assembled. Laser ablation of body wall muscle precursors can lead to a gap in a muscle quadrant. Within this gap, no perlecan accumulates, and within the hypodermis adjacent to the gap, no hemidesmosomes accumulate (Moerman et al., 1996; Hresko et al., 1999). One interpretation of these observations is that muscle is essential for organizing hemidesmosomal complex assembly within the hypodermis. If muscle is acting as an inducer, wider muscle cells may therefore lead to a wider hemidesmosomal complex within the hypodermis.

Our data cannot distinguish between these two models. What our observations do underscore is that during embryogenesis there is a dynamic interaction between muscle and hypodermis to ensure that force transmission from muscle is distributed evenly across the apposing face of the hypodermis. We have shown that spectrin has a critical role in this interaction. Future studies using the power of *C. elegans* and the spectrin mutants may enable us to describe the function of the spectrin cytoskeleton during development in still greater detail.

Materials and methods

Strains, maintenance, and positional cloning of *spc-1*

C. elegans strains were maintained and cultured as described by Brenner (1974). The N2 Bristol strain was used as the control wild-type strain. Unless otherwise indicated, all genetic experiments were performed at 20°C. The following mutant alleles and chromosomal rearrangements were used in this study: *dpy-3(e27)*, *egl-19(st556)*, *let-502(h738)*, *lon-2(e678)*, *mlc-4(or253)*, *sma-1(ru18)*, *unc-2(e55)*, *unc-20(e112ts)*, *unc-70(n493n1171)*, *unc-70(s1639)*, and *syDf1*.

spc-1(ra409) was isolated in a mutant screen designed to identify mutations in genes required for muscle development (KRN and DGM [unpublished data]). The *spc-1(ra409)* mutation was mapped to the X chromosome. To further localize *spc-1*, three factor mapping was conducted. *unc-2 + lon-2/+ spc-1 +* and *dpy-3 + unc-20/+ spc-1 +* animals were generated and allowed to self. 12/48 *Unc-2 non-Lon-2* and 6/51 *Unc-20 non-Dpy-3* recombinants were mutant for *spc-1*, placing *spc-1* between *unc-2* and *unc-20*. Additionally, *spc-1(ra409)* mutants failed to complement the deficiency *syDf1*.

Transgenic strains were generated as described by Mello and Fire (1995). N2 animals were injected with two different cocktails of DNA. The first cocktail consisted of 80 µg/ml of pRF4 (dominant *rol-6* mutation; *rol-6[Su1006dm]*) and 10 µg/ml of M01F12. The second cocktail consisted of 80 µg/ml of pRF4 and 20 µg/ml of DM#214 (subclone of M01F12 containing only the α spectrin ORF).

Molecular biology

PCR was conducted as described by Barstead et al. (1991). DNA sequencing reactions were performed directly on PCR amplified genomic DNA and cDNA clones by using the BRL dsDNA Cycle Sequencing System as described by Rogalski et al. (1993) or by the Nucleic Acid/Protein Service unit at the University of British Columbia. Sequence alignments and comparisons were performed using BLAST (National Center for Biotechnology Information server [Altschul et al., 1997]) and ClustalW (Mac Vector). Exon/intron boundaries were determined by sequencing cDNAs yk205f3, yk44a4, (gifts from Y. Kohara, National Institute of Genetics, Mishima, Japan), cm9a10, DM#455, and PCR-amplified fragments from a cDNA library (a gift from R. Barstead, Oklahoma Medical Research Center, Oklahoma City, OK).

General molecular biological techniques were performed as described in Sambrook et al. (1989). The bacterial strains DH5α (BRL) and XL1-Blue (Stratagene) were used for subcloning and fusion protein expression. To generate the full-length α spectrin clone, a 4.7-kb *Avr II* *SpeI* fragment from the cosmid M01F12 (a gift from A. Coulson, Sanger Center, Hinxton, England) was subcloned into *SpeI*-digested pBluescript (Stratagene) to produce DM#213. Subsequently, a 9.1-kb *SpeI* fragment from the cosmid M01F12 was subcloned into the *SpeI* site of DM#213, producing a clone (DM#214) that contains the full-length *C. elegans* α spectrin gene including 2-kb upstream and 1-kb downstream.

To generate a fusion protein encoding part of the *C. elegans* α spectrin gene, the complete third spectrin repeat plus part of the second and fourth spectrin repeat (amino acids 208–449) encoded by exon 4 was cloned into pGEX 4T-1 to produce DM#215. Specifically, PCR was performed to amplify a 957 base pair region of the fourth exon from genomic DNA. Subsequently, the clone DM#215 was produced by digesting this PCR product with *ApoI*, and the fragment was subcloned into the *EcoRI* site of the pGEX 4T-1 vector (Amersham Pharmacia Biotech).

The production of dsRNA and RNAi were conducted as described in Norman and Moerman (2000). The template used for RNA production was the EST clone yk205f3 and DM#455.

Antibody production

The GST α spectrin fusion protein was produced and purified by the procedure described previously (Smith and Johnson, 1988). To generate polyclonal antisera, two New Zealand white rabbits were injected subcutaneously with purified fusion protein emulsified in Freund's complete adjuvant (~0.5 mg protein/rabbit). Rabbits were boosted by intramuscular injections at 4–6-wk intervals with fusion protein emulsified in Freund's incomplete adjuvant (~0.3 mg protein/rabbit), and blood samples were taken 10–12 d after injection. Immune response was monitored by Western blotting of purified fusion proteins and worm extracts and by immunofluorescence staining of nematodes. Antibodies were affinity purified according to Miller and Shakes (1995). Antibodies were further purified with a bacterial-GST acetone powder that removed all GST reactivity.

Immunofluorescence and microscopy

Embryo fixation, antibody staining, and microscopy were performed as described in Norman and Moerman (2000). Fluorescence microscopy was

conducted on a ZEISS Axiovert equipped with the Radiance 2000 confocal system (Bio-Rad Laboratories, Inc). A minimum of 10 animals was examined for each genotype. Animals were staged according to pharyngeal development. The antibodies used in this study were a mouse monoclonal antibody to myosin heavy chain A (DM5.6 [Miller et al., 1983]), a mouse monoclonal antibody to nematode intermediate filaments (MH4 [Francis and Waterston, 1991]), a rabbit polyclonal to nematode perlecan (GM1 [Moerman et al., 1996]), a rabbit polyclonal to nematode α spectrin (AS1), and a rabbit polyclonal antibody to nematode β spectrin (Moorthy et al., 2000). DM5.6, GM1, and the AS1 were diluted 1:50; MH4 was diluted 1:100; the β spectrin antibody was diluted 1:500. The secondary antibodies used were FITC-labeled donkey anti-rabbit IgG F(ab')₂ and Texas red-labeled donkey anti-mouse IgG F(ab')₂ (Jackson ImmunoResearch Laboratories) and were diluted 1:200. For control, *spc-1(RNAi)* embryos, using yk205f3 and DM#455 for dsRNA production, were labeled with AS1 to test for specificity. Additionally, AS1 antiserum was incubated over night at 4°C with the spectrin-GST fusion protein that was used to generate the AS1 antiserum and stain wild-type embryos. No immunofluorescence signal was detected in these experiments. Embryos for FITC-phalloidin staining were prepared as described by Costa et al. (1997). Differential interference contrast images were collected on a ZEISS Axiovert microscope equipped with differential interference contrast optics. The images were collected using a Dage-MTI CCD-100 digital camera and Scion image software. Adobe Photoshop 4.0® was used to present images. Time-lapse video recording was performed as described by McKeown et al. (1998) except embryos were imaged every 5 s.

We thank J. Culotti for the help in isolating *spc-1(ra417::Tc1)*, the *Caenorhabditis* Genetics Center, D. Baillie, A. Rose, and J. Austin for nematode strains, D. Miller, V. Bennett, and M. Hresko for antibodies, M. Costa for phalloidin staining protocol, J. Bonner for comments on the article, and the anonymous reviewers for numerous suggestions that resulted in a much improved article.

This work was supported by grants from the Canadian Institute for Health Research and the Heart and Stroke Foundation of Canada.

Submitted: 13 November 2001

Revised: 13 March 2002

Accepted: 21 March 2002

References

- Altschul, S.F., T.L. Madden, A.A. Schaffer, J. Zhang, Z. Zhang, W. Miller, and D.J. Lipman. 1997. Gapped BLAST and PSI-BLAST: a new generation of protein database search programs. *Nucleic Acids Res.* 25:3389–3402.
- Barstead, R.J., L. Kleiman, and R.H. Waterston. 1991. Cloning, sequencing, and mapping of an alpha-actinin gene from the nematode *Caenorhabditis elegans*. *Cell Motil. Cytoskeleton.* 20:69–78.
- Bennett, V., and A.J. Baines. 2001. Spectrin and ankyrin-based pathways: metazoan inventions for integrating cells into tissues. *Physiol. Rev.* 81:1353–1392.
- Brenner, S. 1974. The genetics of *Caenorhabditis elegans*. *Genetics.* 77:71–94.
- C. elegans* Sequencing Consortium. 1998. Genome sequence of the nematode *C. elegans*: a platform for investigating biology. *Science.* 282:2012–2018.
- Chin-Sang, I.D., and A.D. Chisholm. 2000. Form of the worm: genetics of epidermal morphogenesis in *C. elegans*. *Trends Genet.* 16:544–551.
- Costa, M., B.W. Draper, and J.R. Priess. 1997. The role of actin filaments in patterning the *Caenorhabditis elegans* cuticle. *Dev. Biol.* 184:373–384.
- de Cuevas, M., J.K. Lee, and A.C. Spradling. 1996. Alpha-spectrin is required for germline cell division and differentiation in the *Drosophila* ovary. *Development.* 122:3959–3968.
- Dubreuil, R., T.J. Byers, D. Branton, L.S. Goldstein, and D.P. Kiehart. 1987. *Drosophila* spectrin. I. Characterization of the purified protein. *J. Cell Biol.* 105:2095–2102.
- Dubreuil, R.R., T.J. Byers, C.T. Stewart, and D.P. Kiehart. 1990. A beta-spectrin isoform from *Drosophila* (beta H) is similar in size to vertebrate dystrophin. *J. Cell Biol.* 111:1849–1858.
- Dubreuil, R.R., P.B. Maddux, T.A. Grushko, and G.R. MacVicar. 1997. Segregation of two spectrin isoforms: polarized membrane-binding sites direct polarized membrane skeleton assembly. *Mol. Biol. Cell.* 8:1933–1942.
- Dubreuil, R.R., P. Wang, S. Dahl, J. Lee, and L.S. Goldstein. 2000. *Drosophila* beta spectrin functions independently of alpha spectrin to polarize the Na,K ATPase in epithelial cells. *J. Cell Biol.* 149:647–656.

- Featherstone, D.E., W.S. Davis, R.R. Dubreuil, and K. Broadie. 2001. *Drosophila* alpha- and beta-spectrin mutations disrupt presynaptic neurotransmitter release. *J. Neurosci.* 21:4215–4224.
- Fire, A., S. Xu, M.K. Montgomery, S.A. Kostas, S.E. Driver, and C.C. Mello. 1998. Potent and specific genetic interference by double-stranded RNA in *Caenorhabditis elegans*. *Nature.* 391:806–811.
- Francis, R., and R.H. Waterston. 1991. Muscle cell attachment in *Caenorhabditis elegans*. *J. Cell Biol.* 114:465–479.
- Hammarlund, M., W.S. Davis, and E.M. Jorgensen. 2000. Mutations in β -spectrin disrupt axon outgrowth and sarcomere structure. *J. Cell Biol.* 149:931–942.
- Hresko, M.C., B.D. Williams, and R.H. Waterston. 1994. Assembly of body wall muscle and muscle cell attachment structures in *Caenorhabditis elegans*. *J. Cell Biol.* 124:491–506.
- Hresko, M.C., L.A. Schriefer, P. Shrimankar, and R.H. Waterston. 1999. Myotactin, a novel hypodermal protein involved in muscle–cell adhesion in *Caenorhabditis elegans*. *J. Cell Biol.* 146:659–672.
- Lee, J.K., E. Brandin, D. Branton, and L.S. Goldstein. 1997a. alpha-spectrin is required for ovarian follicle monolayer integrity in *Drosophila melanogaster*. *Development.* 124:353–362.
- Lee, R.Y., L. Lobel, M. Hengartner, H.R. Horvitz, and L. Avery. 1997b. Mutations in the alpha1 subunit of an L-type voltage-activated Ca²⁺ channel cause myotonia in *Caenorhabditis elegans*. *EMBO J.* 16:6066–6076.
- Lux, S.E., and J. Palek. 1995. Disorders of the red cell membrane. In *Blood: Principles and Practice of Hematology*. R.I. Handin, S.E. Lux and T.P. Stossel, editors. J.B. Lippincott Company, Philadelphia, PA. 1701–1818.
- McKeown, C., V. Praitis, and J. Austin. 1998. *sma-1* encodes a betaH-spectrin homolog required for *Caenorhabditis elegans* morphogenesis. *Development.* 125:2087–2098.
- Mello, C., and A. Fire. 1995. DNA transformation. *Methods Cell Biol.* 48:451–482.
- Miller, D.M., and D.C. Shakes. 1995. Immunofluorescence microscopy. *Methods Cell Biol.* 48:365–394.
- Miller, D.M., III, I. Ortiz, G.C. Berliner, and H.F. Epstein. 1983. Differential localization of two myosins within nematode thick filaments. *Cell.* 34:477–490.
- Moerman, D.G., and A. Fire. 1997. Muscle: structure, function and development. In *C. elegans II*. D.L. Riddle, T. Blumenthal, B.J. Meyer, and J.R. Priess, editors. Cold Spring Harbor Laboratory Press, Cold Spring Harbor, NY. 417–470.
- Moerman, D.G., H. Hutter, G.P. Mullen, and R. Schnabel. 1996. Cell autonomous expression of perlecan and plasticity of cell shape in embryonic muscle of *Caenorhabditis elegans*. *Dev. Biol.* 173:228–242.
- Moorthy, S., L. Chen, and V. Bennett. 2000. *Caenorhabditis elegans* β -G spectrin is dispensable for establishment of epithelial polarity, but essential for muscular and neuronal function. *J. Cell Biol.* 149:915–930.
- Norman, K.R., and D.G. Moerman. 2000. The *let-268* locus of *Caenorhabditis elegans* encodes a procollagen lysyl hydroxylase that is essential for type IV collagen secretion. *Dev. Biol.* 227:690–705.
- Pesacreta, T.C., T.J. Byers, R. Dubreuil, D.P. Kiehart, and D. Branton. 1989. *Drosophila* spectrin: the membrane skeleton during embryogenesis. *J. Cell Biol.* 108:1697–1709.
- Priess, J.R., and D.I. Hirsh. 1986. *Caenorhabditis elegans* morphogenesis: the role of the cytoskeleton in elongation of the embryo. *Dev. Biol.* 117:156–173.
- Rogalski, T.M., B.D. Williams, G.P. Mullen, and D.G. Moerman. 1993. Products of the *unc-52* gene in *Caenorhabditis elegans* are homologous to the core protein of the mammalian basement membrane heparan sulfate proteoglycan. *Genes Dev.* 7:1471–1484.
- Sadler, T.W., K. Burrridge, and J. Yonker. 1986. A potential role for spectrin during neurulation. *J. Embryol. Exp. Morphol.* 94:73–82.
- Sambrook, J., E.F. Fritsch, and T. Maniatis. 1989. *Molecular Cloning: A Laboratory Manual*. Cold Spring Harbor Laboratory Press, Cold Spring Harbor, NY.
- Shelton, C.A., J.C. Carter, G.C. Ellis, and B. Bowerman. 1999. The nonmuscle myosin regulatory light chain gene *mlc-4* is required for cytokinesis, anterior-posterior polarity, and body morphology during *Caenorhabditis elegans* embryogenesis. *J. Cell Biol.* 146:439–451.
- Smith, D.B., and K.S. Johnson. 1988. Single-step purification of polypeptides expressed in *Escherichia coli* as fusions with glutathione S-transferase. *Gene.* 67:31–40.
- Thomas, G.H. 2001. Spectrin: the ghost in the machine. *Bioessays.* 23:152–160.
- Thomas, G.H., and D.P. Kiehart. 1994. Beta heavy-spectrin has a restricted tissue and subcellular distribution during *Drosophila* embryogenesis. *Development.* 120:2039–2050.
- Thomas, G.H., D.C. Zarnescu, A.E. Juedes, M.A. Bales, A. Londergan, C.C. Korte, and D.P. Kiehart. 1998. *Drosophila* betaHeavy-spectrin is essential for development and contributes to specific cell fates in the eye. *Development.* 125:2125–2134.
- Waterston, R.H. 1988. Muscles. In *The Nematode Caenorhabditis elegans*. W.B. Wood, editor. Cold Spring Harbor Laboratory Press, Cold Spring Harbor, NY. 281–336.
- Wessel, G.M., and S.W. Chen. 1993. Transient, localized accumulation of alpha-spectrin during sea urchin morphogenesis. *Dev. Biol.* 155:161–171.
- Williams, B.D., and R.H. Waterston. 1994. Genes critical for muscle development and function in *Caenorhabditis elegans* identified through lethal mutations. *J. Cell Biol.* 124:475–490.
- Wissmann, A., J. Ingles, J.D. McGhee, and P.E. Mains. 1997. *Caenorhabditis elegans* LET-502 is related to Rho-binding kinases and human myotonic dystrophy kinase and interacts genetically with a homolog of the regulatory subunit of smooth muscle myosin phosphatase to affect cell shape. *Genes Dev.* 11:409–422.
- Zarnescu, D.C., and G.H. Thomas. 1999. Apical spectrin is essential for epithelial morphogenesis but not apicobasal polarity in *Drosophila*. *J. Cell Biol.* 146:1075–1086.